

# Phase transformation behavior of nanocrystalline $\chi$ -alumina powder obtained by thermal decomposition of AIP in inert organic solvent

O. MEKASUWANDUMRONG

*Research Center on Catalysis and Catalytic Reaction Engineering, Department of Chemical Engineering, Faculty of Engineering, Chulalongkorn University, Bangkok 10330, Thailand; Department of Energy and Hydrocarbon Chemistry, Graduate School of Engineering, Kyoto University, Kyoto 606-8077, Japan*

P. PRASERTHDAM

*Research Center on Catalysis and Catalytic Reaction Engineering, Department of Chemical Engineering, Faculty of Engineering, Chulalongkorn University, Bangkok 10330, Thailand*  
E-mail: *piyasan.p@chula.ac.th*

M. INOUE

*Department of Energy and Hydrocarbon Chemistry, Graduate School of Engineering, Kyoto University, Kyoto 606-8077, Japan*

V. PAVARAJARN

*Research Center on Catalysis and Catalytic Reaction Engineering, Department of Chemical Engineering, Faculty of Engineering, Chulalongkorn University, Bangkok 10330, Thailand*

W. TANAKULRUNGSANK

*Department of Chemical Engineering, Faculty of Engineering, Rajamangala Institute of Technology, Pathumthani 12110, Thailand*

---

Thermal decomposition of aluminum isopropoxide (AIP) in inert organic solvents (toluene and mineral oil) resulted in the formation of  $\chi$ -alumina. Phase evolution by calcination at various temperatures for this alumina was studied via X-ray diffraction. The results suggest a direct transformation from  $\chi$ -alumina to  $\alpha$ -alumina at approximately 1180°C, without the formation of  $\kappa$ -alumina phase, while still maintaining the small particle size (<100 nm). The transformation behavior was observed by TEM and the crystallite size was calculated by the Scherrer equation. The results indicate one  $\chi$ -alumina crystal transforms into one  $\alpha$ -alumina crystal at its critical size in a nucleation step. This crystal exhibits a rapid grain growth following the transformation. © 2004 Kluwer Academic Publishers

---

## 1. Introduction

Alumina (Al<sub>2</sub>O<sub>3</sub>) is widely used as a catalyst, a support or as a wear-resistance material [1], because of its distinctive chemical, mechanical and thermal properties.  $\chi$ -alumina is a crystallographic form of transition alumina, normally obtained by dehydration of Gibbsite (<200 nm) [2–4]. It transforms into  $\kappa$ -alumina at around 650–750°C with a loss in surface area. Three different unit cells have been suggested for  $\chi$ -alumina: cubic and 2 forms of hexagonal close-packed with different lattice parameters.

Several studies have been carried out on the direct phase transformation of alumina. The mechanism of phase transformation [5, 6] and the direct phase transformation from  $\gamma$ -alumina to  $\alpha$ -alumina involving the conversion of the cubic close packing of oxygen ions into a stable hexagonal close packing have been examined. Others have reported on

methods of enhancing the rate of phase transformation [7–9].

$\chi$ -alumina prepared from thermal decomposition of AIP in inert organic solvents has high thermal stability and directly transforms into  $\alpha$ -alumina at the temperature around 1150°C resulting in no loss in the surface area by the  $\kappa$ -phase formation. Because of the direct phase transformation behavior of  $\chi$ -alumina, nanocrystalline  $\alpha$ -alumina can be obtained. In this paper, we report results for direct  $\alpha$ -phase formation as well as the morphology of alumina before and after the phase transformation as studied by TEM and SEM.

## 2. Experimental

### 2.1. Powder preparation

8 g of Aluminum isopropoxide (AIP) was suspended in 100 ml of inert organic solvent (toluene or mineral oil)

in a test tube, which was then placed in 200 ml autoclave. The gap between the test tube and the autoclave wall was filled with 30 ml of the same solvent. The autoclave was purged by nitrogen and heated up to 315°C at the rate of 2.5°C/min, and held at that temperature for 2 h. After the mixture was cooled down, the resulting product was repeatedly washed with acetone and then dried in air.

To investigate the effect of cations contamination on the phase transformation of  $\chi$ -alumina, the small amounts of sodium tert-butoxide was added in the mixture of AIP and toluene and followed with the above procedure.

A part of the powder was calcined in a box furnace by heating up to the desired temperature (1000–1200°C) at the rate of 10°C/min and holding at that temperature for 1 h.

## 2.2. Characterization

Powder X-ray diffraction (XRD) patterns were obtained with a SIEMENS XRD D5000 diffractometer using Cu  $K_{\alpha}$  radiation. The crystallite size was calculate using the Scherrer equation. The value of shape factor,  $K$ , was taken to be 0.9 and  $\alpha$ -alumina was used as an external standard having the infinity crystallite size. Thermal analyses (TGA and DTA) were performed using a thermal analyzer (Shimadzu TG-50, Shimadzu, Kyoto, Japan) at a heating rate of 10°C/min under a 40 ml/min flow of dry air. Primary particles of alumina samples were observed by a JEOL TEM-200cx transmission electron microscope, operated at 100 kV. Morphologies of the alumina powders were observed using a JEOL scanning electron microscope. BET surface areas were calculated by the BET-single point method on the basis of the nitrogen uptake measured at  $P/P_0 = 0.3$  using a thermal conductivity detector. Surface areas calculated by the conventional BET method were in good agreement with those calculated by the single-point method.

## 3. Results and discussions

XRD patterns of the products, prepared in toluene (TA) and mineral oil (MA) followed by calcination at various temperatures, are shown in Fig. 1a and b respectively. The XRD pattern of the powder obtained by reaction at 315°C for 2 h. shows a peak at  $2\theta = 42.5$ . This peak corresponds to the prohibited (321) diffraction of the spinel structure and it is an indicator of the formation of  $\chi$ -alumina. With increasing calcination temperature, both samples exhibited the XRD patterns corresponding to  $\chi$ -alumina together with small amount of  $\alpha$ -alumina and contamination of our samples by  $\theta$ -alumina, which might be derived from contamination of our sample from by boehmite. The presence of boehmite was confirmed from the IR spectra of samples. The  $\alpha$ -phase transformation was completed at 1180°C. Interestingly,  $\chi$ -alumina obtained from the thermal decomposition of AIP in both solvents transformed to stable  $\alpha$ -alumina directly, bypassing the formation of  $\kappa$ -alumina. In general,  $\chi$ -alumina obtained by dehydration of Gibbsite (<200 nm) transforms

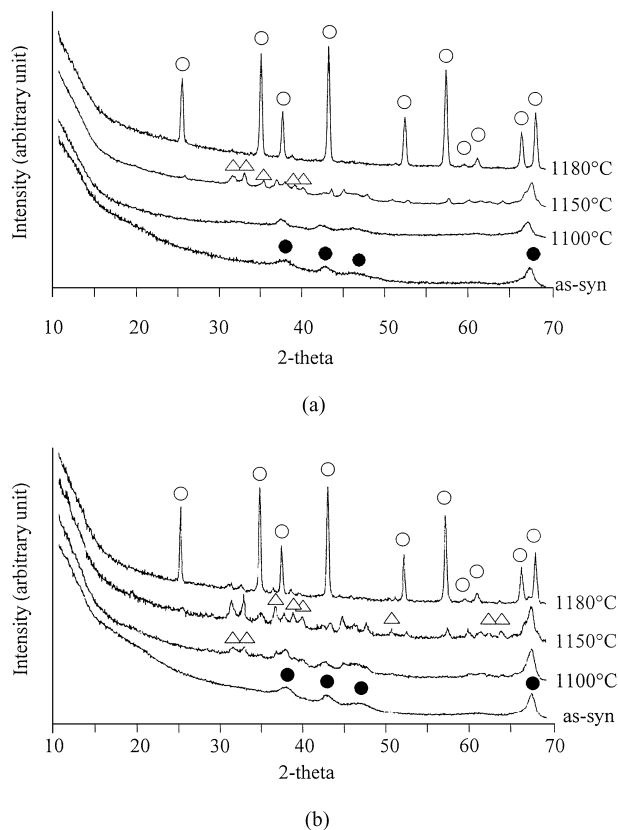


Figure 1 The XRD patterns of alumina products calcined at various temperatures: (a) prepared in toluene and (b) prepared in mineral oil: ● is  $\chi$ -alumina, ○ is  $\alpha$ -alumina and is  $\Delta$   $\theta$ -alumina.

into  $\alpha$ -alumina through  $\kappa$ -alumina in the sequence as follows:

Gibbsite -  $\chi$ -alumina -  $\kappa$ -alumina -  $\alpha$ -alumina.

Direct transformation of a low-temperature transition alumina ( $\chi$ -alumina) into  $\alpha$ -alumina is specific property of alumina formed by thermal decomposition of aluminum alkoxide in inert organic solvent. Gibbsite is always contaminated with a small amount of cations such as  $Na^+$ , and thermal dehydration yielding  $\chi$ -alumina can not eliminate such ions from the matrix. Therefore, the XRD peaks corresponding to  $\chi$ -alumina from the product obtained by calcination of Gibbsite are always weak and obscured because of low crystallinity and many defects in its structure. Several researchers have reported that the addition of cations into the alumina matrix affected the phase transformation behavior [10–13]. Apparently cations in  $\chi$ -alumina matrix promote the formation of  $\kappa$ -alumina at high calcination temperature. On the other hand,  $\chi$ -alumina obtained by the thermal decomposition of AIP in toluene is not contaminated with cations. Moreover, the presence of a small amount of water during the decomposition process increases the crystallinity of the product. This stabilizes the  $\chi$ -alumina structure and prohibits the formation of  $\kappa$ -alumina. It seems that the direct transformation to  $\alpha$ -alumina can be explained by the absence of cations and fewer defects in the crystal structure. The effect of impurity cations was tested by adding  $Na^+$  ions to the alumina matrix (the atomic ratio of

TABLE I The physical properties of as-synthesized products

Sample ID	BET surface area (m <sup>2</sup> /g)	Crystallite size (nm)	Crystallite size at 1180°C (nm)	Bulk density (g/cm <sup>3</sup> )	%Weight loss
TAI	201	10.3	36.5	0.6	14
MAI	178	10.2	107.5	0.36	12

Na/Al = 0.03). The XRD patterns of the powder obtained, calcined at various temperatures, are shown in Fig. 2. It is clearly seen that the  $\chi$ -alumina did not transform directly to  $\alpha$ -alumina at high calcination temperatures. The effect of defects on the transformation behavior has been reported in many papers. Dynys [14] reported that lattice damage in  $\gamma$ -alumina by ball-milling process increased the density of nuclei and the transformation rate of  $\alpha$ -alumina. The physical properties of powders produced are summarized in Table I. It can be seen that the crystallite size of the samples remain smaller than 100 nm, even after calcination at temperature as high as 1180°C.

Thermal analysis results of the as-synthesized products are shown in Fig. 3. Two weight decrease process were detected, both of which were accompanied by endothermic peaks in DTA. The first step at 80°C is attributed to the desorption of physisorbed water. The second step at 100–500°C is attributed to the dehydration of surface hydroxyl groups.

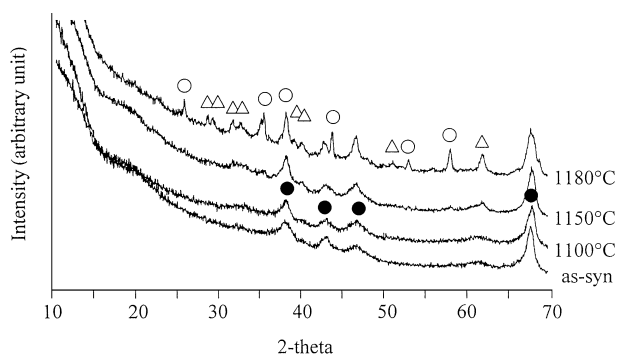


Figure 2 The XRD patterns of alumina with sodium contamination (Na/Al atom = 0.03) products prepared by the reaction of AIP in toluene calcined at various temperatures: ● is  $\chi$ -alumina, ○ is  $\alpha$ -alumina and △ is  $\theta$ -alumina.

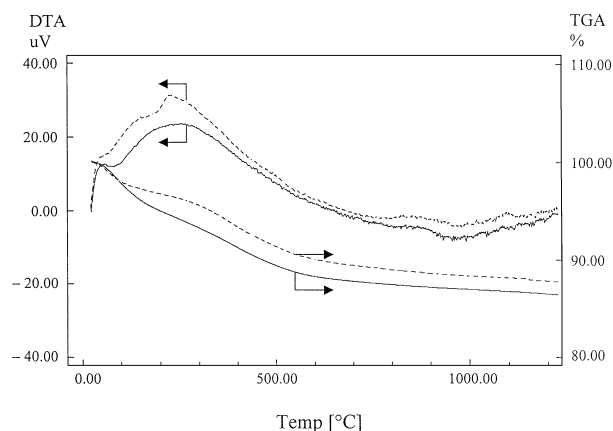


Figure 3 TG and DTA data of the as-synthesized products: (—) prepared in toluene and (---) prepared in mineral oil.

Transmission Electron Micrographs of the as-synthesized and calcined powders prepared in both organic solvents are shown in Fig. 4. The as-synthesized  $\chi$ -alumina powders were comprised of agglomerated primary particles having diameter of 6 to 13 nm. The crystallite sizes of the products from the reaction in toluene and mineral oil, calculated by Scherrer equation were 10.3 and 10.2 nm respectively. The particle size calculated from measured surface area, according to the assumption that the powders consist of uniform spherical particle and have a specific gravity of 3 g/cm<sup>3</sup>, was 10 nm, which is in good agreement with the crystallite size. This suggests that each primary particle observed by TEM is a single crystal of  $\chi$ -alumina. When powders were heated to higher temperature, the size of primary particles increased and these particles were identified as  $\alpha$ -alumina. Interestingly, the TEM images clearly show two different types of the particles in the calcined product: vermicular shape (around 100–200 nm) and a small spherical particle (around 15–25 nm). We believe the latter are a  $\chi$ -alumina at a critical size. At this size a nucleation process within the particle converts it to  $\alpha$ -alumina, the calculated values of which from the Scherrer equation, are summarized in Table II. Generally the mechanism for the transformation of alumina to  $\alpha$ -phase consists of nucleation and followed by accretion growth. During the phase transformation,  $\alpha$ -alumina nuclei occur at certain sites in the matrix of  $\chi$ -alumina, followed by the growth of nuclei into the surrounding matrix. To confirm this argument, the product synthesized in toluene was calcined in various conditions and the crystallite sizes of  $\chi$ -alumina and  $\alpha$ -alumina were measured. Results are summarized in Table II. The results clearly show that the crystallite size of  $\chi$ -alumina grew up from 10 to 16 nm then disappears. These results suggests that  $\chi$ -alumina has a critical size (around 16 nm) beyond which it is unstable and undergoes the phase transformation into the  $\alpha$ - form which grew up drastically and then become sluggish.

From the TEM images, particles having average sizes between 30–100 nm were not detected. This suggests that  $\alpha$ -alumina grows rapidly after direct phase transformation from  $\chi$ -alumina, which might be the result from a sintering process. This rapid growth of  $\alpha$ -alumina has been examined by many researchers [6, 14, 15].

Morphologies of as-synthesized and calcined samples observed by SEM are shown in Fig. 5. It was

TABLE II The crystallite size of the alumina products calcined at various conditions

Sample ID	Calcination temperature (°C)	Calcination time (h)	Crystallite size of $\chi$ -alumina (nm)	Crystallite size of $\alpha$ -alumina (nm)	
TAI	1100	1	10.2	–	
		4	15.2	31.9	
		6	15.4	36	
	1150	1	15.9	28	
	1180	1	–	36.5	
MAI	1100	1	10.2	–	
		1150	1	15.7	21.5
		1180	1	–	107.5

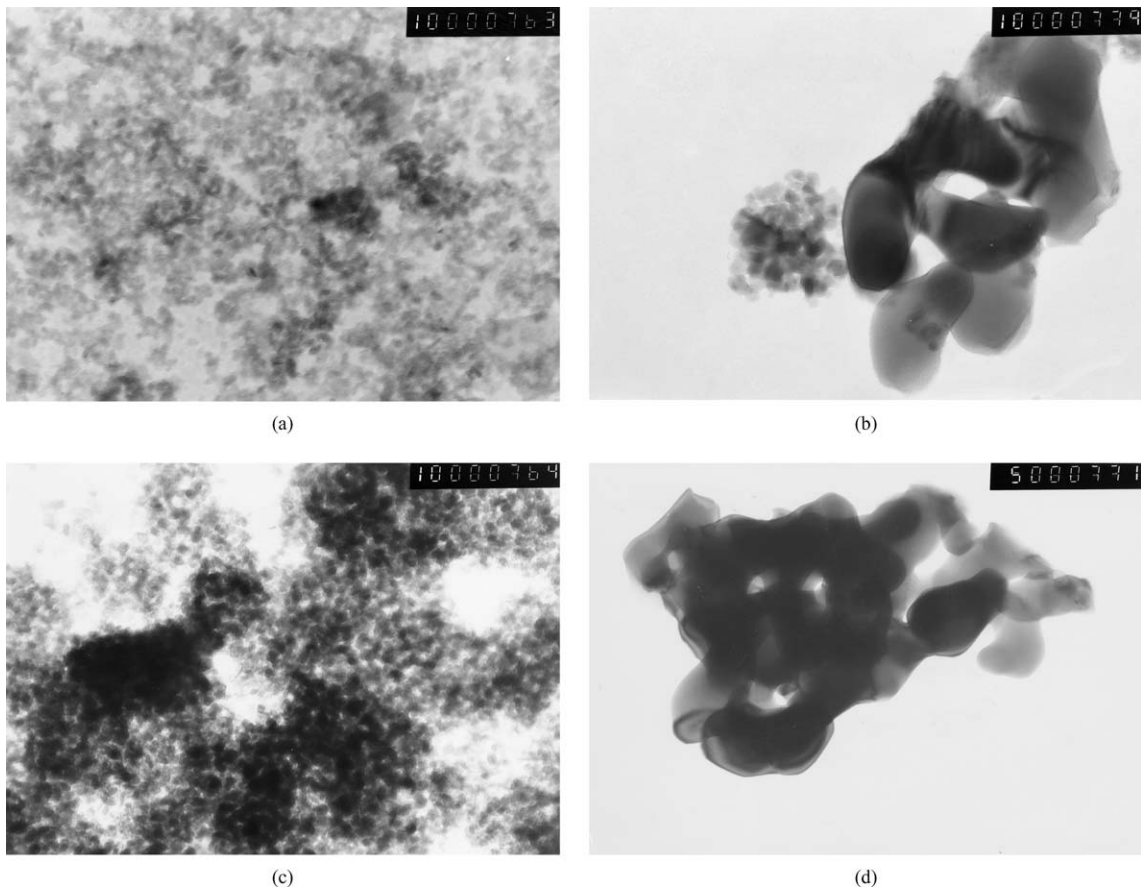


Figure 4 TEM images of alumina products: (a) as-synthesized product prepared in toluene, (b) product prepared in toluene and calcined at 1180°C, (c) as-synthesized product prepared in mineral oil, and (d) product prepared in mineral oil and calcined at 1180°C.

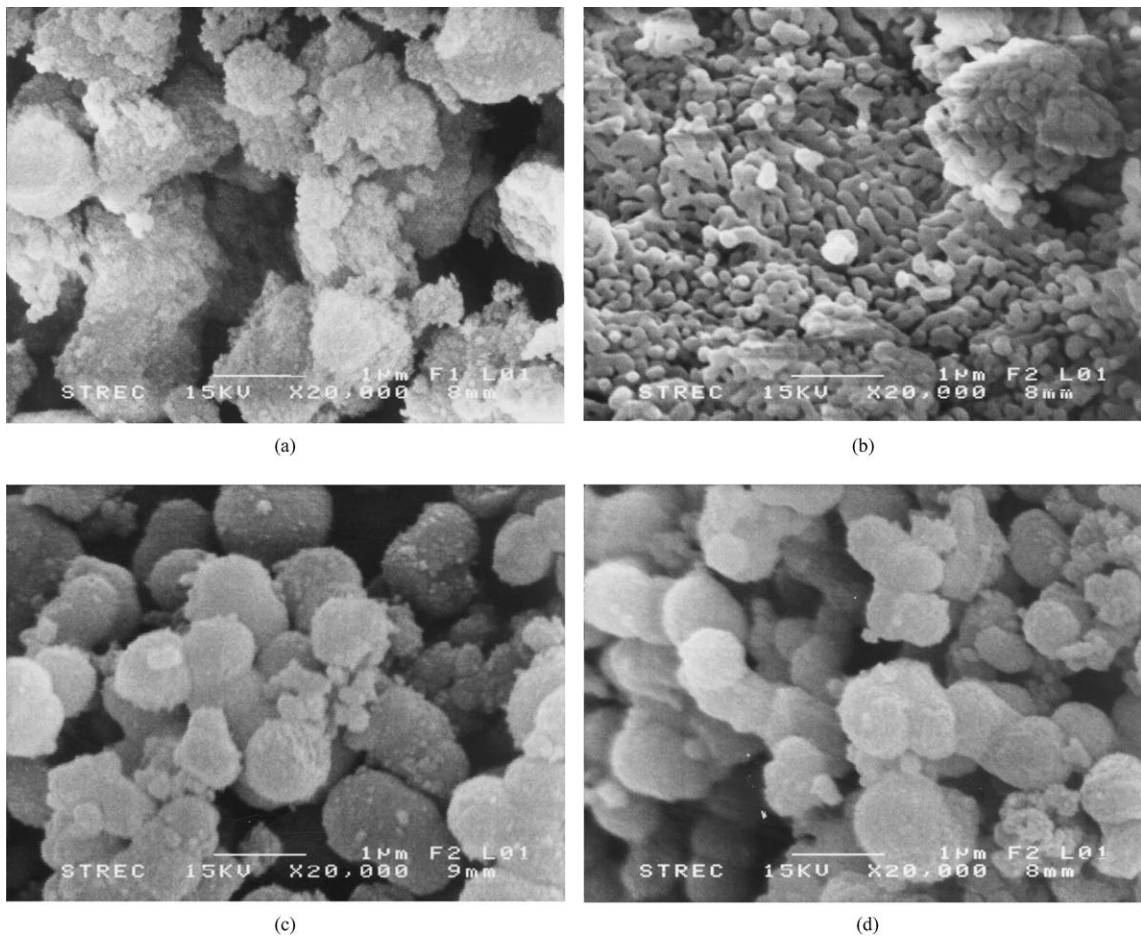


Figure 5 SEM images of alumina products: (a) as-synthesized product prepared in toluene, (b) product prepared in toluene and calcined at 1180°C, (c) as-synthesized product prepared in mineral oil, and (d) product prepared in mineral oil and calcined at 1180°C.

found that the primary particles of powders obtained in mineral oil agglomerated on heating to form bigger and more nearly spherical particles. These particles remained spherical even after the  $\alpha$ -phase transformation. It appears that the  $\alpha$ -phase transformation does not affect the morphologies of particles. On the other hand, in case of reaction in toluene, irregular aggregates made up of nanometer particles are observed (see Fig. 5a). When  $\alpha$ -phase transformation occurred after the aggregates were heated to high temperature, the nano particles have grown significantly and can be identified as individual vermicular particles that are sintered into a large mass.

#### 4. Conclusion

$\chi$ -alumina powders obtained by thermal decomposition of AIP in an inert organic solvent transform to  $\alpha$ -alumina directly without transition through  $\kappa$ -alumina. This direct transformation to  $\alpha$ -alumina can be explained by the absence of cations and fewer defects in the crystal structure. The transformation occurs by nucleation of a  $\chi$ -alumina crystal into a  $\alpha$ -alumina crystal following by the growth of the  $\alpha$ -alumina particles. TEM data indicate that the growth step in the phase transformation is rapid and associated with sintering process.

#### Acknowledgement

The author would like to thank the Thailand Research Fund (TRF), the Thailand-Japan Technology Transfer

Project (TJTTP) for their financial support and Prof. Silveston from Waterloo for assistance in preparing the manuscript.

#### References

1. C. PEREGO and P. L. VILLA, in Proceedings of the 3rd Seminar on Catalysis (Italian Chemical Society, Rimini, Italy, June 1994).
2. H. C. STUMPF, A. S. RUSSELL, J. W. NEWSOME and C. M. TUCKER, *Ind. Eng. Chem.* **42**(7) (1950) 1398.
3. H. SAALFELD, "Structure Phases of Dehydrated Gibbsite," in Reactivity of Solid, edited by J. H. de Boer (Elsevier, Amsterdam, Netherlands, 1961) p. 310.
4. G. W. BRINDLEY and J. O. CHOE, *Amer. Mineral.* **46** (1961) 771.
5. T. W. SIMPSON, Q. Z. WEN, N. YU and D. R. CLARKE, *J. Amer. Ceram. Soc.* **81** (1998) 1995.
6. I. LEVIN and D. BRANDON, *ibid.* **81** (1998) 1995.
7. M. KUMAGAI and G. L. MESSING, *ibid.* **67** (1984) 230.
8. *Idem.*, *ibid.* **67** (1985) 500.
9. L. A. XUE and I. W. CHEN, *J. Mater. Sci. Lett.* **11** (1992) 443.
10. Y. SAITO, T. TAKEI, S. HAYASHI, A. YASUMARI and K. OKADA, *J. Amer. Ceram. Soc.* **81** (1998) 2197.
11. K. OKADA, A. HATTORI, Y. KAMECHIMA and A. YASUMORI, *Mater. Lett.* **42** (2000) 175.
12. K. OKADA, A. HATTORI, Y. KAMECHIMA, A. NUKUI and R. DAS, *J. Amer. Ceram. Soc.* **83** (2000) 928.
13. Y. WU, Y. ZHANG, G. PEZZOTTI and J. GUO, *Mater. Lett.* **52** (2002) 366.
14. F. W. DYNYS and J. W. HALLORAN, *J. Amer. Ceram. Soc.* **65** (1982) 442.
15. R. K. ILLER, *ibid.* **44** (1961) 618.

Received 27 February

and accepted 10 September 2003